Research Square

Preprints are preliminary reports that have not undergone peer review.
They should not be considered conclusive, used to inform clinical practice,
or referenced by the media as validated information.

Spatial-temporally decoupled multi-strain cascade coupled with auxiliary cofactor regeneration for benzylamine bioproduction in Escherichia coli

Jingxin Yin
School of Life Science, Beijing Institute of Technology
Qian Xu
School of Life Science, Beijing Institute of Technology
Chengbin Wang
School of Life Science, Beijing Institute of Technology
Jinli Wang
School of Life Science, Beijing Institute of Technology
Yi An
School of Life Science, Beijing Institute of Technology
Haijun Gao
hj_gao@bit.edu.cn

School of Life Science, Beijing Institute of Technology

Research Article

Keywords: Benzylamine, Auxiliary substrate regeneration, De novo biosynthesis, Multi-strain cascade

Posted Date: November 26th, 2026

DOI: https://doi.org/10.21203/rs.3.rs-11725472/v1

License: This work is licensed under a Creative Commons Attribution 4.0 International License.
Read Full License

Additional Declarations: No competing interests reported.

Spatial-temporally decoupled multi-strain cascade coupled with auxiliary cofactor regeneration for benzylamine bioproduction in *Escherichia coli*

Jingxin Yin[*], Qian Xu[*], Chengbin Wang, Jinli Wang, Yi An[**], Haijun Gao[**]

School of Life Science, Beijing Institute of Technology, Beijing 100081, China

[*]: These authors contributed equally to this work

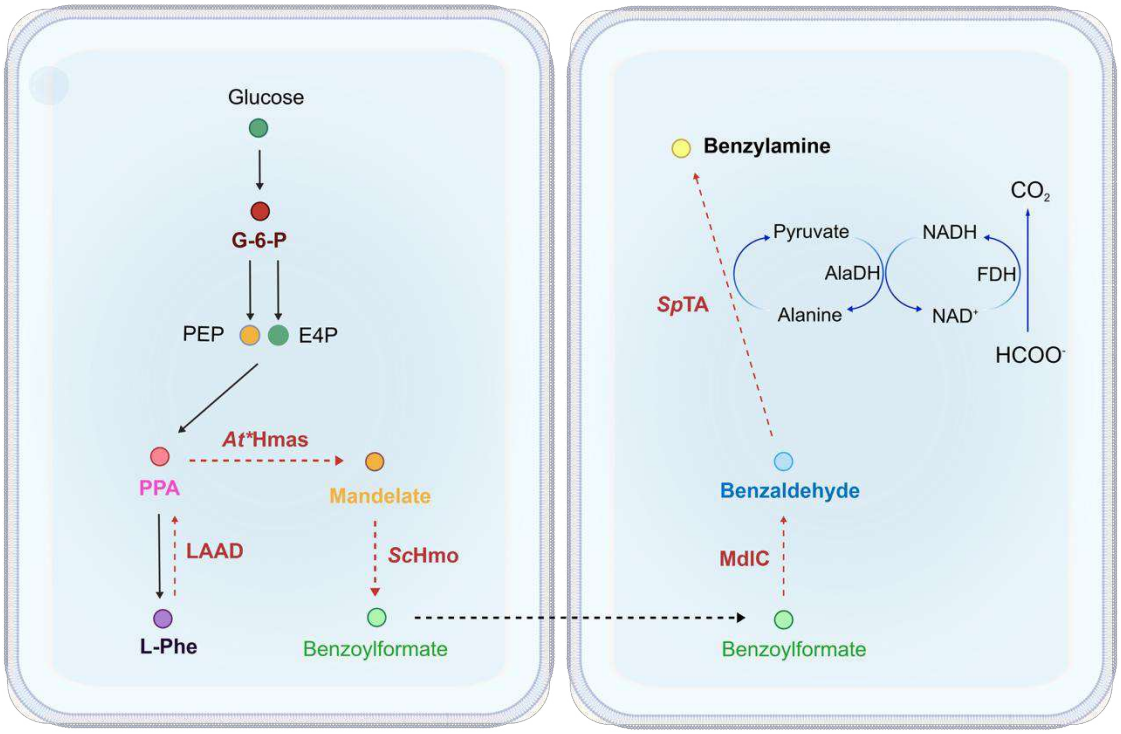
[**]: Corresponding authors

E-mail address: anyi@bit.edu.cn (Y. An), hj_gao@bit.edu.cn (H. Gao)

Abstract: Benzylamine is an important intermediate in the pharmaceutical and chemical industries. To address the environmental and efficiency limitations of traditional chemical synthesis, this study developed an *Escherichia coli* cell factory for the de novo biosynthesis of benzylamine. A four-step heterologous enzyme cascade pathway was designed in the host, featuring phenylpyruvate (PPA) as the pivotal node. To reinforce the precursor supply, carbon flux was redirected by reshaping the central carbon metabolism and the shikimate pathway, while a precursor recovery loop was established via the introduction of an L-amino acid deaminase (LAAD) to minimize intermediate diversion. An alanine and NADH co-regeneration module coupling alanine dehydrogenase and formate dehydrogenase was introduced to shift the unfavorable equilibrium of the PLP-dependent transamination step by removing inhibitory pyruvate and regenerating the amino donor L-alanine. Furthermore, to resolve the physiological oxygen conflict between the aerobic upstream pathway and the downstream transamination operated under sealed conditions, as well as the high volatility of the intermediate benzaldehyde, a multi-strain cascade (MSC) strategy was employed to separate the upstream oxidation and downstream transamination stages. Coupled with high-cell-density resuspension and process optimization, a benzylamine titer of 3.63 mM was achieved from glucose as the primary carbon source without exogenous feeding of aromatic precursors. This study reports the de novo biosynthesis of benzylamine via a multi-strain cascade, and the developed modular assembly, auxiliary substrate regeneration, and process decoupling strategies provide valuable metabolic engineering references for the sustainable biomanufacturing of aromatic amines.

Keywords: Benzylamine; Auxiliary substrate regeneration; De novo biosynthesis; Multi-strain cascade

Graphical abstract



1. Introduction

Benzylamine (C_7H_9N), as a crucial aromatic primary amine, is widely utilized in the pharmaceutical, agrochemical, and polymer industries due to its unique physicochemical properties and biological activities. In the field of polymer materials, benzylamine serves as a core curing agent for high-performance epoxy resins. It constructs a three-dimensional crosslinked network via the crosslinking reaction between its amino and epoxy groups, significantly enhancing the toughness, heat resistance, and chemical stability of the resulting products; notably, the global epoxy curing agent market is predicted to reach USD 6.3 billion by 2030 [1]. In specialty materials, benzylamine-containing ligands are employed as synthetic precursors for the high-energy propellant CL-20, holding vital applications in defense and aerospace sectors [2]. Furthermore, in agrochemistry, it serves as an essential precursor for the insecticide imidacloprid, the herbicide glyphosate, and the plant growth regulator benzyladenine [3, 4]. In pharmaceutical synthesis, benzylamine is not only a key intermediate for the antiepileptic drug lacosamide [5] but is also widely applied in the preparation of antipsychotics and antibacterials [6, 7] showing great promise as a candidate molecule for a new generation of antifungal drugs [7].

Despite this massive demand, traditional chemical synthesis routes for benzylamine still face severe challenges regarding environmental sustainability and synthetic efficiency. The classic reductive amination of benzaldehyde is mature but heavily relies on high-pressure hydrogen gas [8]; the alkaline ammonolysis of benzyl chloride is accompanied by the generation of chlorinated byproducts, imposing a heavy environmental burden [9]; meanwhile, although the catalytic hydrogenation of

benzonitrile is highly efficient, the prohibitive cost of catalyst recovery limits its widespread industrial application [10]. Recently, green synthesis technologies have gained traction. Among them, electrochemical synthesis enables the preparation of benzylamine through the anodic oxidation of benzonitrile while coupling cathodic hydrogen evolution, exhibiting dual advantages in cleanliness and energy efficiency [11]. However, the pervasive issues of insufficient atom economy and toxic waste emissions in chemical methods have driven researchers toward more sustainable biomanufacturing alternatives.

Currently, the enzyme cascade-catalyzed synthesis of benzylamine has attracted extensive attention, with nine-step, four-step, and five-step enzymatic systems reported successively. Zhou et al. [12] first designed a nine-step enzymatic cascade pathway initiating from L-phenylalanine (L-Phe), achieving a 57% yield even in a 100-mL scale reaction. Pandey et al. [13] constructed a four-step cascade pathway via phenylpyruvate (PPA) and mandelate, where the engineered strain synthesized 0.22 mM benzylamine with a conversion rate of 4.5%. Zhu et al. [14] and Wang et al. [15] further optimized five-step enzyme cascades, increasing substrate conversion rates. However, these biosynthetic strategies heavily rely on expensive precursors (such as L-Phe or PPA), significantly driving up raw material costs. Although attempts have been made to establish enzymatic routes, efficient de novo biosynthesis of benzylamine directly from renewable simple carbohydrates, without relying on costly aromatic precursors, still faces significant metabolic hurdles. Core issues, such as the compatibility between the host's endogenous metabolic network and heterologous artificial pathways, the precise

regulation of dynamic metabolic flux, the catalytic efficiency of key enzymes, and cofactor recycling, remain to be deeply elucidated.

In this study, using *Escherichia coli* as the chassis, strategies including pathway design, key enzyme screening, gene expression balancing, precursor supply reinforcement, and auxiliary substrate/cofactor cycling were systematically combined to engineer the strain's metabolic network for the de novo biosynthesis of benzylamine. The major efforts include: modifying the host metabolic network to enhance the supply of precursors L-Phe or PPA; balancing pathway flux through multi-enzyme expression optimization to reduce intermediate accumulation; and constructing an alanine regeneration system coupled with alanine dehydrogenase (AlaDH) and formate dehydrogenase (FDH) to drive auxiliary substrate and cofactor cycling, thereby improving synthetic efficiency. Given the distinct physical and chemical traits of the key intermediate benzaldehyde, we further enhanced final product accumulation through a multi-strain cascade (MSC) and process optimization. This study provides a theoretical foundation and technical support for benzylamine biosynthesis, providing a viable strategy for developing a green and sustainable biomanufacturing system for aromatic amines.

2 Materials and Methods

2.1 Strains, plasmids, and reagents

The strains and plasmids used in this study are listed in Tables S1 and S2. *E. coli* DH5α was used as the host strain for molecular cloning. *E. coli* BL21 RARE, a derivative of BL21 (DE3), was utilized as the host platform for gene expression and benzylamine

biosynthesis. This chassis strain features the genomic deletion of multiple endogenous aldehyde reductase and oxidase genes, which effectively prevents the degradation of volatile aldehyde intermediates, particularly benzaldehyde [16]. All primers used for strain construction are summarized in Table S3 and were synthesized by Sangon Biotech (Shanghai) Co., Ltd. Restriction endonucleases (FastDigest series) were purchased from Thermo Fisher Scientific. Seamless plasmid construction was performed using the ClonExpress Ultra One Step Cloning Kit (Vazyme Biotech Co., Ltd., Nanjing). Chemical reagents and analytical standards were acquired from Sangon Biotech (Shanghai) Co. Ltd. and Sigma-Aldrich Co. Ltd.

2.2 Gene editing and strain construction

Genomic modifications of *E. coli* were performed using the CRISPR-Cas9 system facilitated by the pEcCas and pEcgRNA plasmids[17]. Homologous donor DNA fragments containing target editing templates were prepared via overlap extension PCR. Electrocompetent cells harboring pEcCas (expressing Cas9 and the λ-Red recombinase system) were co-electroporated with the specific pEcgRNA-N20 plasmid and the corresponding donor DNA. Positive transformants were screened on resistance plates and verified by colony PCR. The editing tool plasmids were subsequently cured using rhamnose induction and sucrose-mediated counter-selection.

Heterologous enzyme coding genes (Table S4), including *Pm*LAAD (from *Proteus mirabilis*), *At**HmaS (the engineered 4-hydroxyphenylpyruvate dioxygenase/hydroxymandelate synthase variant A199V/Q206R/I217V/K337Q from *A. teichomyceticus*, encoded by *hppD**, GenBank accession No. BAC68832.1/mutated

according to ref [18]), *Sc*Hmo (from *Streptomyces coelicolor*), MdlC (from *Pseudomonas putida*), *Sp*TA (from *Salicibacter pomeroyi*), AlaDH (encoding alanine dehydrogenase from *B. subtilis*), and *Pse*FDH (from *Pseudomonas* sp. 101), were amplified and cloned into multi-cloning sites of compatible vectors with varying copy numbers (e.g., pCDFDuet-1 and pRSFDuet-1) via Gibson assembly to generate modular expression units.

2.3 Media and cultivation conditions

Seed cultures were prepared by inoculating activated single colonies into Luria-Bertani (LB) medium (10 g/L peptone, 5 g/L yeast extract, and 10 g/L NaCl, pH 7.2) and shaking at 37 °C and 190 r/min for 16 h. For protein expression and fermentation, a 1% (v/v) inoculation volume of the seed culture was transferred into 250-mL Erlenmeyer flasks containing 50 mL of Terrific Broth (TB) medium. The TB medium consisted of 4 mL/L glycerol, 24 g/L yeast extract, 12 g/L peptone, 2.2 g/L KH_2PO_4, and 9.4 g/L K_2HPO_4 (pH 7.2). Recombinant strains were grown at 37 °C and 190 r/min until the OD_{600} reached 0.6–1.0. Protein expression was then induced by adding isopropyl β-D-1-thiogalactopyranoside (IPTG) to a final concentration of 0.2 mM, and the incubation temperature was shifted to 30 °C for an additional 24 h. Antibiotics were added at the following working concentrations as required for plasmid maintenance: spectinomycin (50 μg/mL for pCDF-derived plasmids) and kanamycin (50 μg/mL for pRSF-derived plasmids).

2.4 Whole-cell catalysis for benzylamine synthesis

Resting cell catalysis. Induced cells were harvested by centrifugation, washed twice with sterile distilled water, and resuspended in 100 mM potassium phosphate buffer (pH 7.0) to achieve a standardized cell density (OD_{600} 8.5). The 1-mL reaction mixture was composed of 10–20 mM L-phenylalanine (L-Phe) or alternative pathway precursors, 1 mM pyridoxal phosphate (PLP), 10 mM L-alanine (L-Ala), 100 mM NH_4^+, and 2 g/L glucose. The bioconversion was conducted in 12-mL aerated tubes at 30 °C and 220 r/min for 24 h.

Growing cell catalysis. Concurrently with the addition of 0.2 mM IPTG during the exponential growth phase, substrate and auxiliary substrates at the aforementioned concentrations were directly supplemented into the culture broth, followed by cultivation at 30 °C for 24 h.

2.5 Single-stage benzylamine biosynthesis without aromatic precursor addition

For *de novo* biosynthesis, engineered strains were cultivated in TB medium supplemented with an initial 20 g/L glucose upon IPTG induction, fermentations were maintained at 30 °C and 220 r/min for 24–48 h with intermittent feeding of 2 g/L glucose every 12 h as indicated. To maintain metabolic activity, the culture pH was periodically adjusted to 7.0 using aqueous ammonia.

2.6 Two-Stage Fermentation Strategies

Single-strain two-stage fermentation. Cultivation was performed in a 250-mL Erlenmeyer flask with a working volume of 50-mL. In the first (aerobic) stage, the engineered strain A-12 was grown under basic conditions. Upon IPTG induction, the

broth was supplemented with 20 g/L glucose, 10 mM L-alanine, 100 mM NH_4Cl, 10 mM sodium formate, and 1 mM PLP. The flask was incubated under aerobic conditions (breathable closure) at 30 °C and 220 r/min for 24 h. In the second (sealed bioconversion) stage, the flask was sealed tightly with a sterile airtight rubber stopper to prevent intermediate volatilization and incubated for an additional 24 h. Every 12 h, 2 g/L glucose was injected into the sealed flask via a syringe to maintain cell viability, and the pH was regulated at 7.0 using aqueous ammonia.

Multi-strain cascade (MSC) two-stage fermentation. Strains A-13 and A-14 were cultivated and induced in separate individual cultures. In the first stage, strain A-13 was cultured aerobically in TB medium containing 20 g/L glucose at 30 °C for 24 h to maximize the accumulation of the intermediate benzoylformate. The fermentation broth was then centrifuged to discard the A-13 cell pellet, and the supernatant was collected. The cell-free supernatant was subsequently fortified with 10 mM L-alanine, 100 mM NH_4Cl, 10 mM sodium formate, and 1 mM PLP. For the second stage, induced cells of strain A-14 were harvested and resuspended in this supplemented supernatant to reach an OD_{600} of 25. The flask was immediately sealed with a sterile rubber stopper and incubated at 30 °C and 220 r/min for 24 h, with 2 g/L glucose injected via a syringe every 12 h.

2.7 Analytical methods

Cell density was monitored by measuring the optical density at 600 nm (OD_{600}) using a spectrophotometer.

Quantitative analysis of metabolic intermediates and the final product was performed using an Agilent 1260 Infinity II High-Performance Liquid Chromatography (HPLC) system [15]. Chromatographic separation was executed on a GL Sciences InertSustain C18 column (4.6 mm × 250 mm × 5 μm). The mobile phase consisted of 0.1% trifluoroacetic acid (TFA) in water and acetonitrile (80:20, v/v) operated at a constant flow rate of 0.5 mL/min. The column temperature was maintained at 35 °C, and compounds were detected by UV absorbance at 210 nm with an injection volume of 10 μL. This method allowed simultaneous separation and quantification of benzylamine, L-Phe, PPA, mandelate, benzoylformate, and benzaldehyde. Target compounds (PPA, mandelate, benzoylformate, benzaldehyde, and benzylamine) were definitively identified and calibrated against high-purity commercial standards (Sigma-Aldrich). The identity of the enzymatic conversion product from PPA was verified by matching retention times and UV spectra with authentic unsubstituted mandelate standard via spiked co-injection. Target concentrations were calculated using standard calibration curves derived under identical chromatographic conditions.

2.8 Yield and Conversion Calculations

The molar yield ($Y_{P/S}$) of benzylamine–from glucose was defined and calculated based on total glucose supplied:

$$Y_{P/S(total)} = \frac{n_{benzylamine,final}}{n_{glucose,initial} + n_{glucose,fed}}$$

where n represents the total molar amount of substance in the respective fermentation volume.

To evaluate whole-cell bioconversions from exogenous precursors (e.g., L-Phe or PPA to benzylamine), the substrate conversion rate was defined as:

$$\text{Conversion}\ (\%) = (C_{benzylamine}\ /C_{precursor,initial}) \times 100\%$$

All definitions, denominators, and substrate backgrounds are specified explicitly in the respective text and figure legends.

3. Results and discussion

3.1 Pathway design for the *de novo* synthesis of benzylamine

This study aimed to construct an engineered *E. coli* strain capable of *de novo* biosynthesis of benzylamine through systematic metabolic engineering, eliminating the need for exogenous aromatic precursor (e.g., L-Phe or PPA) supplementation. The artificial pathway designed for this route is illustrated in Figure 1. This biosynthetic route consists of two primary segments: the phenylpyruvate (PPA) biosynthetic pathway and the downstream PPA-to-benzylamine conversion cascade. The upstream PPA supply was established by systematically rewiring the host's endogenous metabolic network. Upstream, glucose metabolism feeds into the Embden-Meyerhof-Parnas (EMP) and pentose phosphate (PP) pathways to supply phosphoenolpyruvate (PEP) and erythrose-4-phosphate (E4P), respectively. These two precursors condense to form 3-deoxy-D-arabino-heptulosonate-7-phosphate (DAHP), which enters the shikimate pathway to drive the robust synthesis of PPA.

The downstream conversion of PPA to benzylamine is mediated by an engineered heterologous enzyme cascade, which sequentially employs four key foreign enzymes. An engineered hydroxymandelate synthase (*At**HmaS, also known in gene annotations as

mutated 4-hydroxyphenylpyruvate dioxygenase, HppD*) capable of accepting non-hydroxylated phenylpyruvate to yield mandelate; mandelate oxidase (Hmo); benzoylformate decarboxylase (MdlC); and ω-transaminase (ω-TA). This artificial cascade sequentially transforms PPA via mandelate, benzoylformate, and benzaldehyde intermediates into the target product, benzylamine. In the downstream cascade, the conversion of benzaldehyde to benzylamine is catalyzed by a PLP-dependent ω-transaminase (ω-TA) using L-alanine as the amino donor. To alleviate the unfavorable equilibrium and coproduct inhibition of the transamination step, an auxiliary alanine/NADH co-regeneration loop comprised of AlaDH and FDH was designed (Figure 1C).

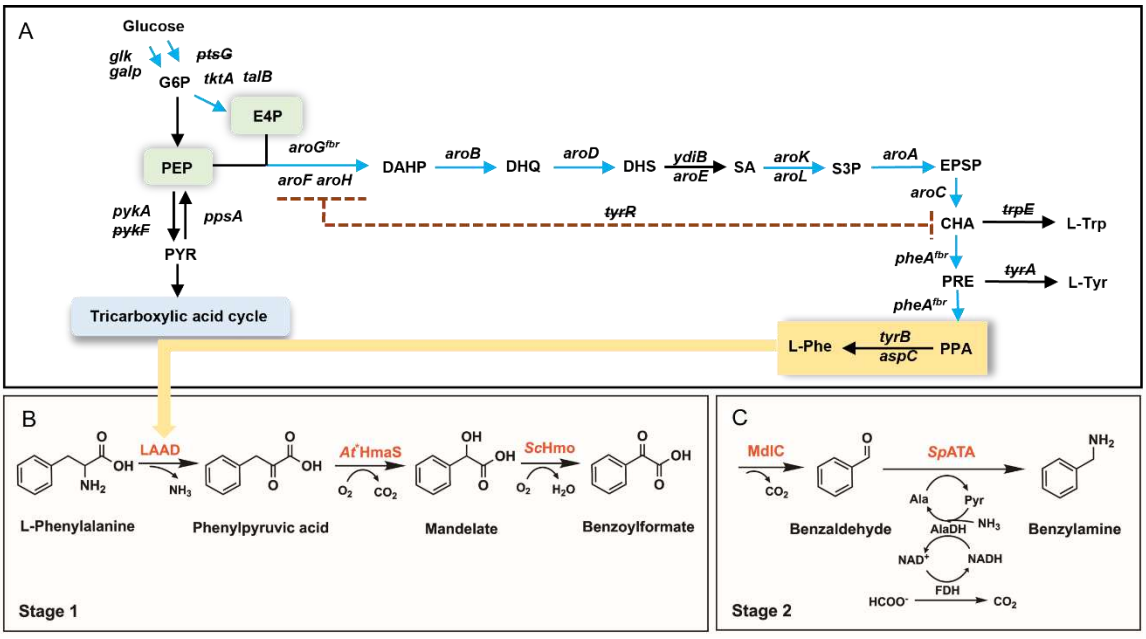


Figure 1. Schematic diagram of the artificial metabolic network designed for the *de novo* biosynthesis of benzylamine in engineered *E. coli*. The integrated pathway is structurally divided into two major segments: A. the upstream endogenous

phenylpyruvate (PPA) biosynthetic module. B. and C. the downstream heterologous PPA-to-benzylamine conversion cascade coupled with an auxiliary substrate and cofactor recycling system, which was split into two expression modules.

Thick light-blue arrows represent enhanced metabolic flux achieved via host genome engineering, while dashed lines or crossed lines indicate blocked competitive pathways or disrupted regulatory mechanisms. Heterologous enzymes driving the non-native cascade are highlighted in bold red font.

Gene or enzyme definitions: *glk,* glucokinase; *galP*, galactose/H^+ symporter (glucose facilitator); *ptsG,* glucose-specific phosphotransferase enzyme IIBC; *tktA*, transketolase A; *aroG*, DAHP synthase (Phe-regulated); *aroF*, DAHP synthase (Tyr-regulated); *aroH*, DAHP synthase (Trp-regulated); *aroB*, 3-Dehydroquinate synthase; *aroD*, 3-Dehydroquinate dehydratase; *ydiB*/*aroE*, shikimate dehydrogenase; *aroK*/*aroL*, shikimate kinase I/II; *aroA*, 5-enolpyruvylshikimate-3-phosphate synthase; *aroC*, chorismate synthase; *tyrR*, TyrR dual transcriptional regulator; *trpE*, anthranilate synthase component I; $pheA^{fbr}$, feedback-resistant chorismate mutase/prephenate dehydratase mutant; *tyrA*, prephenate dehydrogenase (Tyr-regulated); *tyrB*, aromatic aminotransferase; *aspC*, aspartate aminotransferase; *pykA*/*pykF*, pyruvate kinase II (fructose-1,6-bisphosphate-activated); *ppsA,* phosphoenolpyruvate synthetase. LAAD, L-amino acid deaminase; HmaS, 4-hydroxymandelate synthase (or engineered 4-hydroxyphenylpyruvate dioxygenase/mandelate synthase variant, HppD); Hmo, mandelate oxidase; MdlC, benzoylformate decarboxylase; ω-TA, ω-transaminase; AlaDH, alanine dehydrogenase; FDH, formate dehydrogenase. Metabolite abbreviations: G6P, glucose-6-phosphate; E4P, erythrose-4-phosphate; PEP, phosphoenolpyruvate; PYR,

pyruvate; DAHP, 3-deoxy-D-arabino- heptulosonate-7-phosphate; DHQ, 3-dehydroquinate; DHS, 3-dehydroshikimate; SA, shikimate; S3P, shikimate-3-phosphate; EPSP, 5-enolpyruvylshikimate-3-phosphate; CHA, chorismate; PRE, prephenate; PPA, phenylpyruvate; L-Phe, L-phenylalanine; L-Tyr, L-Tyrosine; L-Trp, L-Tryptophan.

3.2 Construction and optimization of the pathway from PPA to benzylamine

To validate the feasibility of the downstream heterologous PPA-to-benzylamine conversion cascade, the four core heterologous enzymes (*Ao*HmaS, *Sc*Hmo, MdlC, and *Sp*TA; Table S4) were co-expressed in *E. coli* BL21 RARE, yielding the initial evaluation strain T-00. Whole-cell catalytic performance was subsequently evaluated using 10 mM of PPA, mandelate, benzoylformate, or benzaldehyde as individual substrates. As shown in Figure 2, all tested intermediates were successfully converted to benzylamine, confirming the functional viability of the artificial route. However, when PPA was supplied as the sole substrate, 2.36 mM of PPA remained unconverted, accompanied by the side-production of 1.53 mM L-Phe. This phenomenon implied that the catalytic efficiency of the selected *Ao*HmaS was relatively limited, whereas the host's endogenous transaminases exhibited a strong competitive metabolic flux that diverted PPA toward L-Phe. Additionally, approximately 1.50 mM of benzaldehyde accumulated as a residual intermediate regardless of the initial substrate utilized, indicating that the transamination activity of the ω-TA represented another critical bottleneck requiring further optimization.

306 To mitigate substrate loss caused by the competitive conversion of PPA to L-Phe, an
307 L-amino acid deaminase (LAAD) was introduced to establish a precursor recovery loop
308 capable of reconverting L-Phe back into PPA. As demonstrated in Figure 2, the resulting
309 strain T-00-1 (expressing LAAD) achieved a benzylamine titer of 5.62 mM from PPA
310 (condition e), representing a 2.2-fold increase compared to that of strain T-00 (condition
311 a) under identical conditions. This result verified that the implementation of the
312 LAAD-mediated recovery loop effectively enhanced the net driving force toward
313 benzylamine by recycling the channeled precursor flux.

314 To systematically relieve the catalytic bottlenecks imposed by HmaS and ω-TA, we
315 screened enzyme candidates from alternative sources. For HmaS evaluation, whole-cell
316 bioconversion was conducted using 10 mM PPA as the substrate in a 1-mL reaction
317 system supplemented with 0.1 mM Fe^{2+} (30 °C, 220 r/min, 24 h) to assess the capability
318 of different HmaS variants in transforming PPA to mandelate [19]. The results (Figure
319 3A) revealed that the HmaS variant *At**HmaS (harboring A199V/Q206R/I217V/K337Q
320 mutations, encoded by the engineered *hppD** gene) derived from *Actinoplanes*
321 *teichomyceticus* [18] exhibited the highest relative activity, achieving a PPA conversion
322 rate of 77.6%, which was 1.6-fold higher than that of its wild-type counterpart. Although
323 canonical wild-type HmaS preferentially acts on 4-hydroxyphenylpyruvate to yield
324 4-hydroxymandelate, structural and biochemical studies by Takakura et al.[18] have
325 established that introducing these four substitutions remodels the active-site pocket into
326 an optimized hydrophobic cavity. This eliminates the steric and electrostatic requirement
327 for the phenolic hydroxyl group, enabling the enzyme to efficiently accept
328 non-hydroxylated phenylpyruvate (PPA) as a substrate and predominantly catalyze its

transformation into unsubstituted mandelate. The identity of the formed mandelate intermediate in our bioconversion assays was verified by C18 HPLC comparison against a commercial authentic mandelate standard (co-eluting with identical retention times and UV absorption profiles, distinct from 4-hydroxymandelate). Meanwhile, the *Ao**HmaS mutant (S201V) from *Amycolatopsis orientalis* [20] yielded a conversion rate of 70.2% (a 7.1-fold increase over wild-type *Ao*HmaS) due to the substitution of a hydrophobic residue that increases substrate affinity [21]. Based on these outcomes, *At**HmaS was selected for further strain engineering.

Concurrently, the catalytic performances of four ω-transaminases—*Sp*TA (from *Salicibacter pomeroyi*), *Vf*TA (from *Vibrio fluvialis*), *Bm*TA (from *Bacillus megaterium*), and *Ad*TA (from *Alcaligenes denitrificans*)—were compared using 10 mM benzaldehyde as the substrate and 20 mM L-alanine as the amino donor [22]. As shown in Figure 3B, *Sp*TA displayed the highest relative activity, driving a benzylamine conversion rate of up to 86.9%.

To further fine-tune the total pathway flux, modular expression cascades were compartmentalized into modular expression units using compatible vectors (pACYCDuet-1, pCDFDuet-1, pETDuet-1, and pRSFDuet-1) spanning a range of copy numbers (~10, 20, 40, and 100, respectively) [23]. Whole-cell bioconversion profiles demonstrated that harmonizing plasmid copy numbers was crucial to mitigating cellular metabolic burden while maximizing product accumulation. Specifically, when Module 1 (comprising *At**HmaS, LAAD, and *Sc*Hmo) was harbored on the medium-copy plasmid pCDFDuet-1, and Module 2 (comprising MdlC and *Sp*TA) on the high-copy plasmid pRSFDuet-1, the resulting strain T-04 achieved a maximum benzylamine titer of 6.59

mM from 10 mM initial L-Phe (Figure 4), corresponding to a substrate molar conversion of 65.9%. Under these conditions, pathway intermediates and residual substrate were: 0.65 mM unreacted L-Phe/PPA, 0.08 mM mandelate, 0.04 mM benzoylformate, and 0.38 mM benzaldehyde, giving a 77.4% aromatic ring mass balance recovery; the unrecovered fraction may stem from intermediate volatilization into the headspace, potential trace side-metabolites, and operational sample losses during extraction. Thus, this optimal vector combination (pCDF-LHS1 and pRSF-SM0) was selected for subsequent *de novo* pathway integration.

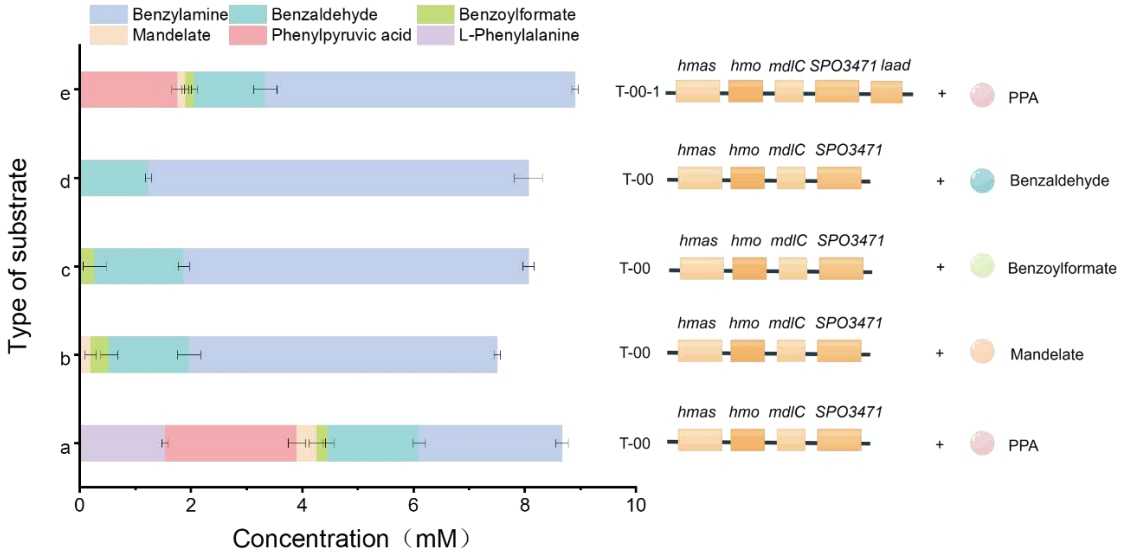


Figure 2. Benzylamine biosynthesis from various upstream precursors and intermediates via whole-cell bioconversion. Recombinant strain T-00 was systematically tested using 10 mM of PPA (a), mandelate (b), benzoylformate (c), or benzaldehyde (d) as individual substrates to assess the baseline pathway efficiency. Condition (e) showcases the enhanced bioconversion efficiency achieved by strain T-00-1 (co-expressing LAAD) using 10 mM PPA as the precursor. Bioconversion assays were

carried out at 30 °C and 220 r/min for 24 h with a cell density of OD_{600} 8.5. Error bars represent the standard deviations (SD) calculated from three independent biological replicates.

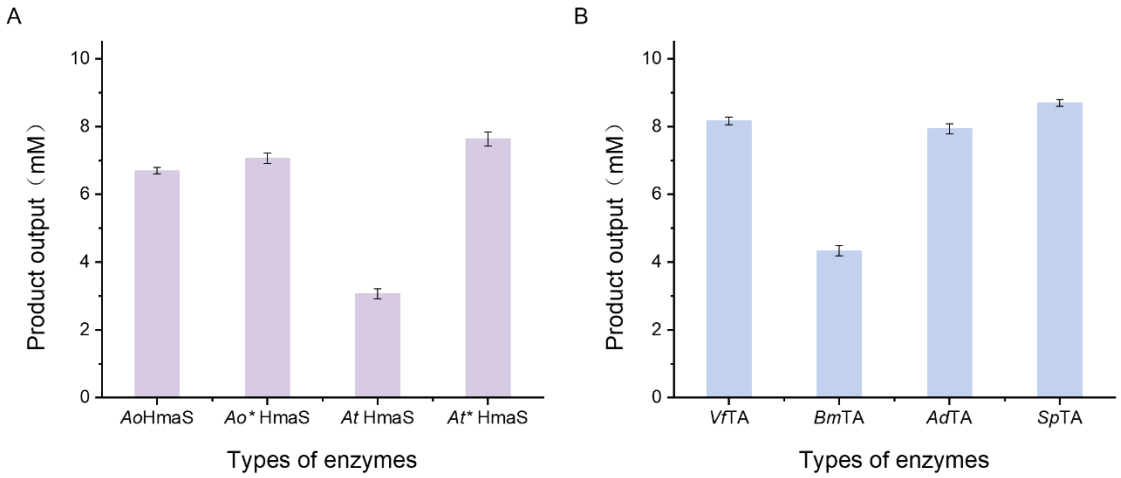


Figure 3. Screening and evaluation of catalytic performances of HmaS and ω-TA variants from alternative sources. (A) Bioconversion efficiencies of different HmaS variants transforming PPA to mandelate. The 1-mL reaction mixture contained 10 mM PPA and 0.1 mM Fe2+. (B) Bioconversion efficiencies of different ω-TA variants transforming benzaldehyde to benzylamine. The 1-mL reaction mixture was composed of 10 mM benzaldehyde and 20 mM L-alanine as the amino donor. All assays were performed using resting cells normalized by biomass to a standardized optical density (OD600 8.5) at 30 °C and 220 r/min for 24 h. Error bars represent the standard deviations (SD) calculated from three independent biological replicates.

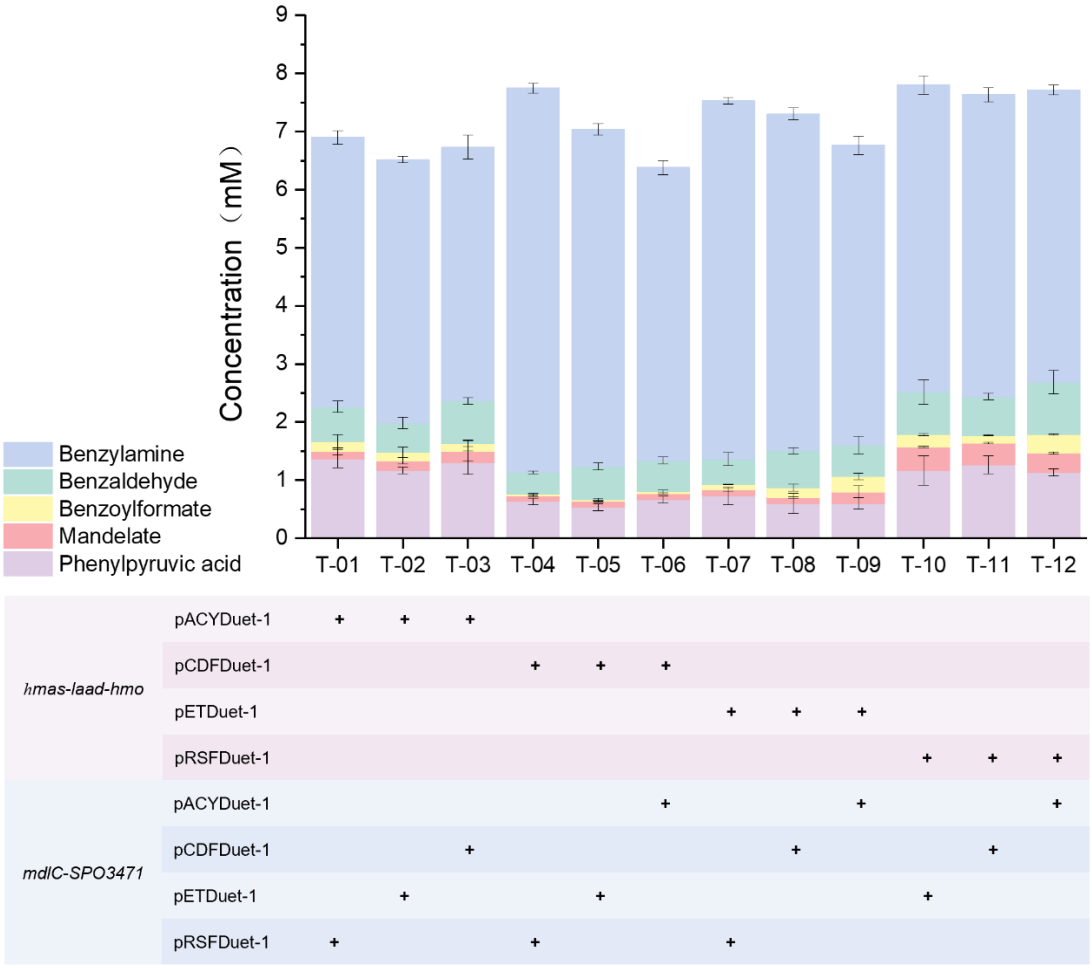


Figure 4. Optimization of modular pathway expression using various plasmid combinations to enhance benzylamine synthesis. The five-enzyme heterologous cascade converting L-Phe to benzylamine was partitioned into two expression blocks: Module 1 (comprising *At**HmaS, LAAD, and *Sc*Hmo) and Module 2 (comprising MdlC and *Sp*TA). A series of recombinant strains (T-01 to T-12) were constructed by pairing compatible vectors (pACYCDuet-1, pCDFDuet-1, pETDuet-1, and pRSFDuet-1) possessing a gradient of copy numbers (~10, 20, 40, and 100, respectively). The matrix table below the plot defines the specific plasmid vector paired for each engineered strain (+ indicates presence). Whole-cell bioconversion was performed in a 1-mL reaction system

containing 10 mM L-Phe (exogenous substrate), 20 mM L-alanine, and 2 g/L glucose at 30 °C and 220 r/min for 24 h using resting cells (OD_{600} 8.5). Strain T-04 delivered the maximum benzylamine titer of 6.59 mM, representing a molar substrate conversion of 65.9% based on initial fed L-Phe (6.59 mM / 10 mM). The stacked bars reflect the direct quantification of benzylamine along with detectable residual substrates and intermediates (PPA, mandelate, benzoylformate, and benzaldehyde) to illustrate intermediate accumulation and total aromatic balance. Error bars represent standard deviations (SD) derived from three independent biological replicates.

3.3 Metabolic engineering of chassis strains to enhance the aromatic pathway biosynthetic capacity

To explore the feasibility of *de novo* benzylamine biosynthesis, we systematically engineered the central metabolic network and the shikimate pathway of the host strain *E. coli* BL21 RARE to enhance carbon flux into the aromatic amino acid branch. In *E. coli*, free PPA is chemically labile and is rapidly transaminated to L-Phe by endogenous aminotransferases (e.g., TyrB and AspC), making steady-state intracellular PPA pools difficult to quantify accurately in long-term batch fermentations [24]. Therefore, L-Phe accumulation by the chassis strains (lacking the downstream heterologous conversion module) was monitored as an indirect operational indicator to assess the host's overall biosynthetic capacity for driving carbon through the shikimate pathway toward aromatic intermediates. Subsequently, the downstream conversion modules were transformed into these engineered chassis to evaluate how effectively this enhanced aromatic pool could be accessed for target product synthesis. The systematic optimization strategies primarily

involved reshaping the glucose transport pathway, alleviating feedback inhibition, eliminating competitive branching pathways, expanding carbon partitioning toward the shikimate pathway, and dynamically strengthening the shikimate pathway itself [25-28] (Figure 1 and 5A). To alleviate the persistent metabolic drag associated with multi-plasmid expression, all overexpressed upstream genes were stably integrated into the host genome, yielding a series of engineered chassis strains designated B-00 through B-07.

The specific impact of each progressive modification on L-Phe synthesis was initially quantified (Figures 5C). The fermentation profiles revealed that L-Phe production exhibited a stepwise increase with the accumulation of genomic modifications. Specifically, the baseline engineered strain B-04 accumulated 21.61 mM L-Phe. Further replacement of the native glucose phosphotransferase system (PTS) with the GalP/Glk transport system (strain B-05) minimized the obligatory consumption of phosphoenolpyruvate (PEP) [29], thereby boosting the L-Phe titer to 30.33 mM. Disruption of the pyruvate kinase gene *pykF* (strain B-06) effectively locked more PEP flux within the aromatic amino acid biosynthetic route. Capitalizing on this background, the targeted overexpression of the transketolase gene *tktA* (strain B-06) or the co-overexpression of *talB* and *tktA* (strain B-07) was executed to expand the availability of the second precursor, erythrose-4-phosphate (E4P). This combinatorial optimization pushed the L-Phe titers to peak values of 37.41 mM and 38.44 mM for strain B-06 and B-07 at 48 h, respectively.

However, evaluating the combined pathway revealed a divergence between upstream precursor capacity and downstream product synthesis. Although the baseline

chassis B-06 and B-07 accumulated substantial titers of L-Phe in the absence of downstream plasmids, the resulting combined strains A-06 and A-07 yielded only ca. 0.25 mM benzylamine (Figure 5D). This discrepancy indicates that a high upstream flux toward aromatic branch does not directly yield accessible phenylpyruvate for the downstream cascade, as endogenous aminotransferases (e.g., TyrB and AspC) divert PPA into the L-Phe pool. Furthermore, the multi-plasmid burden and potential catalytic bottlenecks limit overall pathway throughput, indicating that dedicated strategies to liberate locked intermediates and optimize auxiliary regeneration are required.

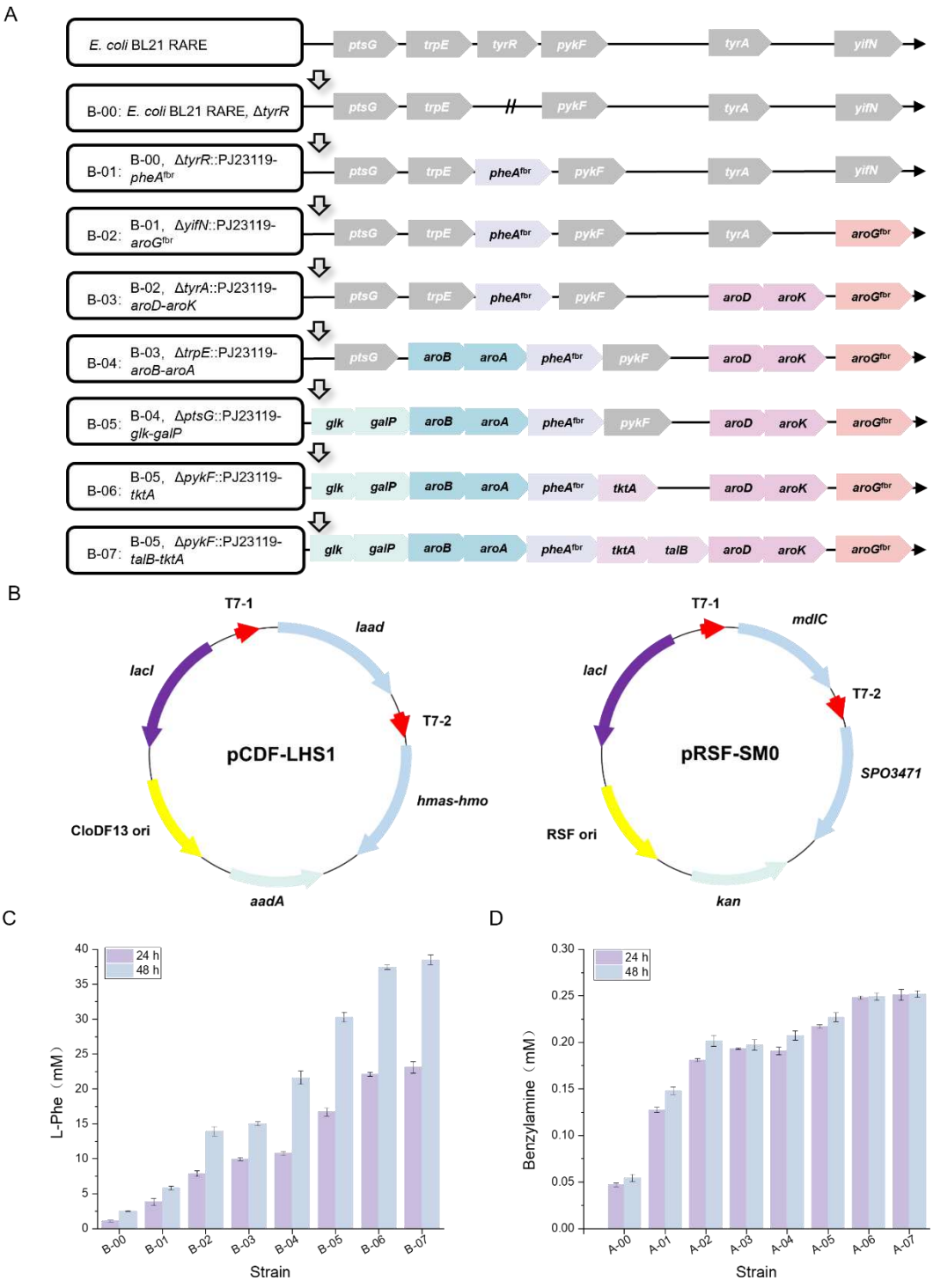


Figure 5. Combinatorial metabolic engineering of *E. coli* chassis and heterologous pathways for the *de novo* biosynthesis of benzylamine. (A) Schematic diagram of the

stepwise genomic modifications in chassis strains (B-00 to B-07) designed to augment carbon flux through the aromatic pathway, including rewriting the glucose transport system (*galP*/*glk*), disrupting competing pathways (*pykF*), and overexpressing the shikimate pathway (*tktA*/*talB*/*aroB*/*aroA*/*pheA*^{fbr}/*aroD*/*aroK*/*aroG*^{fbr}). (B) Plasmid maps of the modular expression vectors pCDF-LHS1 (carrying *hmaS*, *laad*, and *hmo*) and pRSF-SM0 (carrying *mdlC* and *SPO3471*) used for downstream cascade conversion. (C) Evaluation of upstream biosynthetic capacity, showing L-Phe accumulation in engineered chassis strains B-00 to B-07 (without downstream conversion plasmids) during glucose-supplemented batch fermentation. (D) Benzylamine titers produced by recombinant strains A-00 to A-07, generated by introducing pCDF-LHS1 and pRSF-SM0 into the respective B-series chassis. Fermentations were performed in 50-mL TB medium supplemented with 20 g/L initial glucose at 30 °C and 220 r/min for 48 h, with 2 g/L glucose intermittently supplemented every 12 h.

3.4 Engineering of coordinated auxiliary substrate and cofactor regeneration systems

The terminal reductive amination of benzaldehyde into benzylamine is catalyzed by the PLP-dependent transaminase *Sp*TA, using L-alanine (L-Ala) as the amino donor. This reaction is inherently limited by unfavorable equilibrium thermodynamics and severe coproduct inhibition by pyruvate. Although *Sp*TA itself relies on the PLP prosthetic group rather than pyridine nucleotides, the coupled regeneration of L-Ala from pyruvate catalyzed by alanine dehydrogenase (AlaDH) strictly consumes NADH. To relieve

pyruvate inhibition and supply continuous amino donor equivalents without stoichiometric addition, an auxiliary substrate and cofactor co-regeneration cascade was integrated (Figure 1C). In this design, *Bs*AlaDH converts coproduct pyruvate back into L-Ala, while the concomitant reduction of NAD+ to NADH is driven by the irreversible oxidation of formate to CO_2 catalyzed by FDH [30].

To evaluate this strategy, the *ald* gene (encoding *Bs*AlaDH from *Bacillus subtilis*) and the *fdh* gene (encoding *Pse*FDH from *Pseudomonas* sp. 101 or its established high-activity variant, designated *Pse**FDH) were co-expressed in strain A-09 (harboring only the base conversion pathway), yielding recombinant strains A-10 and A-11, respectively. The performance of these co-regeneration systems was systematically evaluated via growing-cell bioconversion using benzaldehyde as the substrate in a medium supplemented with exogenous L-Ala and sodium formate. As demonstrated in Figure 6A, in whole-cell bioconversion feeding 20 mM benzaldehyde in the presence of 10 mM initial L-Ala and 10 mM sodium formate, strain A-10 (expressing wild-type *Pse*FDH) accumulated 15.39 mM benzylamine compared to 13.68 mM in the A-09 control lacking the regeneration module. Furthermore, strain A-11 (harnessing the engineered *Pse**FDH variant with higher specific activity) improved the titer to 16.78 mM.

Based on these findings, this complete, coordinated L-alanine and NADH recycling loop was retrofitted into the genome-engineered chassis strain A-06, successfully generating the *de novo* synthesis strain A-12. Upon evaluating strain A-12 in glucose-fed fermentation, a benzylamine titer of 0.41 mM was obtained after 48 h (Figure 6B), representing a 64% improvement compared to the control strain A-06 (0.25 mM; Figure

5D). These results indicate that co-expressing the AlaDH–FDH module significantly promotes benzylamine accumulation, which is correlated with the intended auxiliary substrate and cofactor regeneration capability.

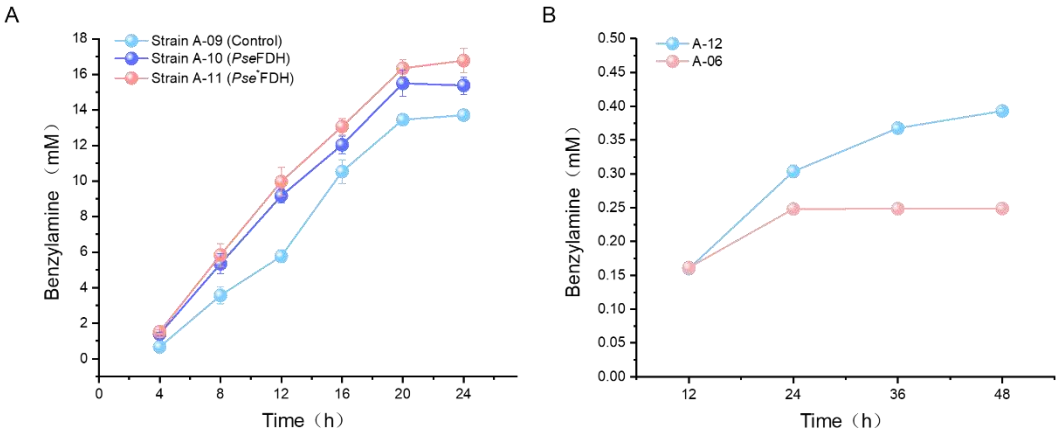


Figure 6. Benzylamine synthesis profiles upon coupling the AlaDH-FDH auxiliary substrate and cofactor regeneration module. (A) Whole-cell bioconversion of benzaldehyde to benzylamine by strain A-09 (base pathway control), strain A-10 (co-expressing *Bs*AlaDH and wild-type *Pse*FDH), and strain A-11 (co-expressing *Bs*AlaDH and high-activity mutant *Pse**FDH). Bioconversions were conducted in 12-mL aerated tubes at 30 °C and 220 r/min for 24 h. The 1-mL reaction mixture contained 20 mM benzaldehyde, 10 mM L-alanine, 100 mM NH_4Cl, 10 mM sodium formate, and 1 mM PLP, with an initial cell density (OD_{600}) adjusted to 25. (B) Time-course profiles of *de novo* benzylamine accumulation in glucose fermentation by strain A-12 (containing the AlaDH-*Pse**FDH module) compared to control strain A-06. Fermentation was performed in a 50-mL working volume containing 20 g/L glucose, 10 mM L-alanine, 100 mM NH_4Cl, 10 mM sodium formate, and 1 mM PLP at 30 °C and 220 r/min for 48 h.

Error bars represent the standard deviations (SD) calculated from three independent biological replicates.

3.5 Development and optimization of a multi-strain cascade process

In the artificial benzylamine biosynthetic pathway, the volatile and chemically reactive nature of the key intermediate, benzaldehyde, presents a severe engineering bottleneck, as it is highly prone to gas stripping under continuous aeration or irreversible oxidation into benzoic acid upon exposure to ambient air [31]. This volatility leads to an unstable precursor supply and severely restricts the downstream substrate conversion efficiency. Conversely, the upstream *de novo* segments—encompassing glucose-to-PPA scaling, L-Phe synthesis, and the subsequent *At**HmaS- and Hmo-catalyzed pathways—are strictly oxygen-dependent aerobic processes. To resolve the physiological conflict between the high-aeration requirements of the upstream module and the sealed-flask environment necessitated by the downstream transamination cascade, we developed a multi-strain cascade (MSC) fermentation strategy. This process achieves a two-stage operational decoupling: the first stage leverages aerated cultivation to drive carbon flux from glucose toward benzoylformate accumulation, while the second stage transitions to a strictly sealed configuration to facilitate the quantitative conversion of benzoylformate to benzylamine, thereby arresting the evaporative loss of the benzaldehyde intermediate.

To initially evaluate the efficacy of this process decoupling, a single-strain, two-stage fermentation system was verified using the engineered strain A-12, which harbors the complete *de novo* pathway alongside the integrated L-alanine/NADH

regeneration loop. The sequential process consisted of a 24-h aerobic cell-growth phase followed by a 24-h sealed bioconversion phase. As illustrated in Figure 7, this single-strain two-stage strategy yielded a benzylamine titer of 1.02 mM, representing a 2.5-fold increase over the single-stage cultivation profile (0.41 mM; Figure 6B).

Based on this improvement, we further advanced the bioprocess by implementing a dual-strain MSC framework. The upstream strain A-13 (carrying pCDF-LHS1) was dedicated exclusively to the aerobic synthesis of L-Phe and its subsequent conversion to benzoylformate, while the downstream strain A-14 (carrying pRSF-SMAF1) was engineered to convert benzoylformate into benzylamine, under sealed-flask conditions while driving the dynamic L-alanine and NADH regeneration cycles. Upon implementing this dual-strain MSC system, the benzylamine titer increased to 2.21 mM (with a molar yield ($Y_{p/s}$) of 0.015 mol benzylamine per mol of total glucose supplied), representing a 2.1-fold improvement over the single-strain two-stage fermentation counterpart (1.02 mM, $Y_{p/s}$=0.007 mol/mol; Figure 7A). This process improvement in the MSC configuration reflects the integrated benefits of spatial-temporal phase separation, fresh cofactor supplementation, and the ability to intensify downstream biocatalyst loading via high-density cell resuspension (ca. OD_{600} 25). Through systematic fine-tuning of the resuspended downstream cell density and process parameters, the final benzylamine titer was improved to 3.63 mM (0.025 mol/mol based on total glucose supplied. Figure S1).

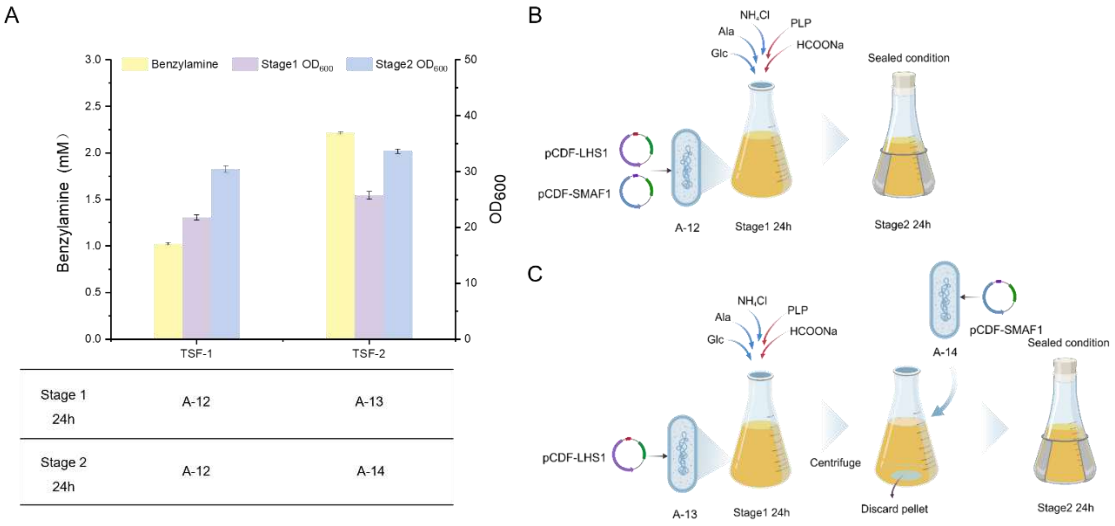


Figure 7. Comparison of *de novo* benzylamine biosynthesis between single-strain and dual-strain MSC two-stage fermentations. **(A)** Benzylamine titers and cell growth (OD_{600}) under different fermentation configurations. TSf-1 represents the single-strain two-stage fermentation using strain A-12. TSf-2 represents the dual-strain MSC two-stage fermentation using strains A-13 and A-14. **(B)** Schematic workflow of the single-strain two-stage fermentation process. Strain A-12 was cultivated under aerobic conditions (breathable closure) for the first 24 h, followed by a 24-h bioconversion phase in a sealed environment. **(C)** Schematic workflow of the dual-strain MSC two-stage fermentation process based on spatial-temporal segregation. In the first stage, strain A-13 was cultured under aerated conditions for 24 h to accumulate benzoylformate, after which cells were removed. In the second stage, induced cells of strain A-14 were resuspended in the supplemented cell-free supernatant (OD_{600} 25) and incubated under sealed conditions for another 24 h. All cultivation profiles utilized a 50-mL initial working volume containing 20 g/L glucose, 10 mM L-alanine, 100 mM NH_4Cl, 10 mM sodium formate,

571 and 1 mM PLP at 30 °C and 220 r/min, with a 2 g/L glucose feeding regimen maintained
572 every 12 h. Error bars represent the standard deviations (SD) calculated from three
573 independent biological replicates.
574
575 **4 Discussion**
576 Addressing the limitations of traditional chemical synthesis and complex multi-step
577 enzymatic cascades, this study established the *de novo* biosynthesis of benzylamine from
578 glucose by rewiring the host metabolic network and introducing a spatial-temporally
579 decoupled bioprocess. In this artificial route, phenylpyruvate (PPA) serves as the central
580 metabolic hub, enabling a four-step catalytic cascade. However, in engineered *E. coli*,
581 free PPA is chemically labile and subject to rapid transamination into L-Phe by
582 endogenous aminotransferases (such as TyrB and AspC), leading to competitive carbon
583 diversion toward L-Phe [24] [28].. This sink effect explains the pronounced discrepancy
584 between the high upstream L-Phe capacity observed in chassis B-06/B-07 and the
585 negligible initial benzylamine yield in the integrated strain A-06. Introducing the
586 LAAD-mediated salvage loop effectively mitigate this precursor diversion by
587 reconverting accumulated L-Phe back into PPA, thereby restoring the net driving force
588 toward the downstream pathway. Nonetheless, the overall throughput is still constrained
589 by the catalytic efficiency of HmaS on non-hydroxylated phenylpyruvate, highlighting
590 the necessity for further protein engineering [18].
591 Another major challenge in artificial amine pathways lies in the unfavorable
592 thermodynamic equilibrium of the transamination step and severe coproduct inhibition by
593 pyruvate [22]. It should be emphasized that while the ω-transaminase *Sp*TA relies strictly

on the PLP prosthetic group and does not directly consume reducing equivalents, the coupled enzymatic recycling of the amino donor L-alanine from pyruvate via AlaDH requires a stoichiometric supply of NADH. Under intense metabolic flux, cofactor availability can become a critical limiting factor. Coupling the AlaDH cascade with formate dehydrogenase (FDH) effectively shifts the overall transamination equilibrium forward by continuously consuming inhibitory pyruvate while regenerating L-alanine [30]. Although direct profiling of the intracellular NADH/NAD^+ ratio and transamination intermediate pools remains to be performed in future studies to fully dissect the *in vivo* kinetics, the stepwise improvement in benzylamine accumulation across strains expressing wild-type and engineered FDH variants is consistent with the hypothesis that auxiliary cofactor driving forces substantially relieve downstream thermodynamic bottlenecks.

At the bioprocess level, the high volatility and chemical instability of the intermediate benzaldehyde pose a prominent barrier, predisposing the process to severe carbon loss under continuous aeration [31]. This physical trait conflicts fundamentally with the physiological requirements of the pathway: the upstream generation of PPA and oxygenase-catalyzed conversions (HmaS and Hmo) require vigorous aeration, whereas the downstream transamination benefits from an oxygen-limited or sealed environment to arrest benzaldehyde evaporation and preserve reducing equivalents. The multi-strain cascade (MSC) fermentation strategy resolves this contradiction by partitioning the multi-enzyme cascade between an aerobic intermediate-producing strain (A-13) and a downstream conversion strain (A-14) [32] [33]. Crucially, the substantial titer improvement achieved in the MSC system over the single-strain two-stage process

reflects an integrated bioprocess outcome rather than pathway compartmentalization alone. It encompasses multiple synergistic factors, including the mitigation of multi-plasmid metabolic burden, tailored microenvironments for oxygen-conflicting enzymes, and the operational flexibility to intensify biocatalyst loading via high-density cell resuspension (OD_{600} approximately 25). Quantitative flux analysis will be required to deconvolute the precise contribution of each individual parameter.

Although this work demonstrates the viability of *de novo* benzylamine biomanufacturing, several engineering hurdles must be overcome to reach industrial metrics. First, the catalytic turnover and stability of HmaS on non-native substrates must be augmented via directed evolution to alleviate intermediate accumulation [18]. Second, benzaldehyde possesses limited aqueous solubility and may impose physiological stress at elevated concentrations. Future bioprocess improvements could incorporate *in situ* two-phase extractive fermentation systems (using biocompatible organic solvents or resin adsorbents) to dynamically sequester benzaldehyde and the accumulated benzylamine product, thereby mitigating cellular toxicity and preventing volatilization. Finally, integrating dynamic metabolic control, such as autonomous genetic circuits or degron tags, could dynamically shut down competing amino acid transamination during the production phase [32], maximizing carbon routing from renewable feedstocks toward target aromatic amines.

5 Conclusion

In this study, an engineered *E. coli* cell factory was developed for the *de novo* biosynthesis of benzylamine directly from glucose as the primary carbon source without exogenous aromatic precursor supplementation. By rewiring the host shikimate pathway

and deploying an artificial four-step cascade centered on phenylpyruvate, a dedicated precursor-recovery loop mediated by an exogenous L-amino acid deaminase (LAAD) was established to effectively counteract endogenous transamination and unlock sequestered precursor flux. To overcome thermodynamic equilibrium barriers and pyruvate coproduct inhibition during downstream transamination, an intracellular auxiliary substrate and cofactor co-regeneration module coupling alanine dehydrogenase and formate dehydrogenase was successfully implemented. Furthermore, a two-stage multi-strain cascade (MSC) fermentation strategy with an aeration-then-sealing configuration successfully resolved the physiological conflict between upstream oxygen demand and downstream intermediate benzaldehyde volatility, while allowing high-density downstream biocatalyst loading. Consequently, a final benzylamine titer of 3.63 mM was achieved from glucose, corresponding to a molar yield of 0.025 mol/mol based on total glucose supplied and 0.031 mol/mol based on glucose consumed. Overall, this integrated framework combining modular chassis engineering, auxiliary substrate regeneration, and bioprocess decoupling provides a viable biomanufacturing route for benzylamine and offers valuable architectural references for the sustainable synthesis of other value-added aromatic compounds.

ASSOCIATED CONTENT

Supporting Information

Strains used in this study (Supplemental Table S1), plasmids used in this study (Supplemental table S2), primer used in this study (Supplemental Table S3), genes used

in engineered *E. coli* in this study (Supplemental Table S4). Time-course profiles of *de novo* benzylamine biosynthesis via the optimized two-stage MSC fermentation (Supplemental Figure S1).

Acknowledgments

The authors would like to acknowledge the Biological & Medical Engineering Core Facilities, School of Life Science, Beijing Institute of Technology for the equipment and technical support.

Authors' Contributions

J.Y.: Performed methodology, investigation, visualization, and original draft. Q.X.: Performed conceptualization, validation, visualization, and writing –original draft, review & editing. C.W. and J.W.: Performed methodology, investigation, manuscript revision. Y.A.: Performed conceptualization, formal analysis, writing – original draft. H.G.: Performed conceptualization, supervision, writing –original draft, review & editing.

Funding

Funding sources are listed in the "Acknowledgements".

Availability of data and materials

All data generated or analyzed during this study are included in this published article and its additional files.

Ethics approval and consent to participate

Not applicable.

Consent for publication

Not applicable.

Notes

The authors declare no competing financial interest.

AUTHOR INFORMATION

Corresponding Authors

Yi An, School of Life Science, Beijing Institute of Technology, Beijing 100081, China; Email: anyi@bit.edu.cn

Haijun Gao, School of Life Science, Beijing Institute of Technology, Beijing 100081, China; Email: hj_gao@bit.edu.cn

Authors

Jingxin Yin, School of Life Science, Beijing Institute of Technology, Beijing 100081, China; Email: yinjingxin04@163.com

Qian Xu, School of Life Science, Beijing Institute of Technology, Beijing 100081, China; Email: 3120251441@bit.edu.cn

Chengbin Wang, School of Life Science, Beijing Institute of Technology, Beijing 100081, China; Email: 384825230@qq.com

Jinli Wang, School of Life Science, Beijing Institute of Technology, Beijing 100081, China; Email: wjl1128qx@163.com

References

1. Data Bridge Market Research. Global epoxy curing agents market - Industry trends and forecast to 2030. Research DBM. 2023. http://doi.org:https://www.databridgemarketresearch.com/reports/global-epoxy-curing-agents-market

2. Nair UR, Sivabalan R, Gore GM, Geetha M, Asthana SN, Singh H. Hexanitrohexaazaisowurtzitane (CL-20) and CL-20-based formulations (Review). Combust Explos Shock Waves. 2005, 41(2):121–132. http://doi.org:10.1007/s10573-005-0014-2

3. Dolezal K, Popa I, Hauserová E, Spíchal L, Chakrabarty K, Novák O, Krystof V, Voller J, Holub J, Strnad M. Preparation, biological activity and endogenous occurrence of N6-benzyladenosines. Bioorg Med Chem. 2007, 15(11):3737–3747. http://doi.org:10.1016/j.bmc.2007.03.038

4. Sardoei AS, Tahmasebi M, Bovand F, Ghorbanpour M. Exogenously applied gibberellic acid and benzylamine modulate growth and chemical constituents of dwarf schefflera: a stepwise regression analysis. Sci Rep. 2024, 14(1):7896. http://doi.org:10.1038/s41598-024-57985-0

5. Morieux P, Stables JP, Kohn H. Synthesis and anticonvulsant activities of N-benzyl (*2R*)-2-acetamido-3-oxysubstituted propionamide derivatives. Bioorg Med Chem. 2008, 16(19):8968–8975. http://doi.org:10.1016/j.bmc.2008.08.055

732 6. Cuisiat S, Bourdiol N, Lacharme V, Newman-Tancredi A, Colpaert F, Vach
733 er B. Towards a new generation of potential antipsychotic agents combinin
734 g D2 and 5-HT1A receptor activities. J Med Chem. 2007, 50(4):865–876. h
735 ttp://doi.org:10.1021/jm061180b
736 7. Krauss J, Stadler M, Bracher F. Synthesis and structure-activity relationship
737 s of novel benzylamine-type antifungals as butenafine-related antimycotics.
738 Arch Pharm. 2017, 350(5). http://doi.org:10.1002/ardp.201600342
739 8. Gomez S, Peters JA, van der Waal JC, Zhou W, Maschmeyer T. Preparati
740 on of benzylamine by highly selective reductive amination of benzaldehyde
741 over Ru on an acidic activated carbon support as the catalyst. Catal Lett.
742 2002, 84(1):1–5. http://doi.org:10.1023/A:1021068432604
743 9. Krupka J, Dluhoš L, Mrózek L. Evaluation of benzylamine production via
744 reductive amination of benzaldehyde in a slurry reactor. Chem Eng Technol.
745 2017, 40(5):870–877. http://doi.org:10.1002/ceat.201600538
746 10. Hao Y, Li M, Cárdenas-Lizana F, Keane MA. Selective production of benz
747 ylamine via gas phase hydrogenation of benzonitrile over supported Pd cata
748 lysts. Catal Lett. 2016, 146(1):109–116. http://doi.org:10.1007/s10562-015-16
749 55-8
750 11. Reziguli Y, Kadierya A, Luo S, Abulikemu AR. Synthesis of N-benzyliden
751 e benzylamine from dibenzylamine and derivatization under electrochemical

conditions. Acta Chim Sin. 2024, 82(8):843–848. http://doi.org:10.6023/A24040119

12. Zhou Y, Wu S, Mao J, Li Z. Bioproduction of benzylamine from renewable feedstocks via a nine-step artificial enzyme cascade and engineered metabolic pathways. ChemSusChem. 2018, 11(13):2221–2228. http://doi.org:10.1002/cssc.201800709

13. Pandey RP, Casini A, Voigt CA, Gordon DB. Four-step pathway from phenylpyruvate to benzylamine, an intermediate to the high-energy propellant CL-20. ACS Synth Biol. 2021, 10(9):2187–2196. http://doi.org:10.1021/acssynbio.1c00021

14. Zhu Y, Yang T, Chen Y, Fan C, Yuan J. One-pot synthesis of aromatic amines from renewable feedstocks via whole-cell biocatalysis. ChemistrySelect. 2020, 5(45):14292–14295. http://doi.org:10.1002/slct.202003807

15. Wang J, Dong R, Yin J, Liang J, Gao H. Optimization of multi-enzyme cascade process for the biosynthesis of benzylamine. Biosci Biotechnol Biochem. 2023, 87(11):1373–1380. http://doi.org:10.1093/bbb/zbad111

16. Butler ND, Anderson SR, Dickey RM, Nain P, Kunjapur AM. Combinatorial gene inactivation of aldehyde dehydrogenases mitigates aldehyde oxidation catalyzed by *E. coli* resting cells. Metab Eng. 2023, 77:294–305. http://doi.org:10.1016/j.ymben.2023.04.014

17. Li Q, Sun B, Chen J, Zhang Y, Jiang Y, Yang S. A modified pCas/pTargetF system for CRISPR-Cas9-assisted genome editing in *Escherichia coli*. Acta Biochim Biophys Sin. 2021, 53(5):620–627. http://doi.org:10.1093/abbs/gmab036

18. Takakura Y, Ono T, Danjo K, Nozaki H. Efficient enzymatic production of benzaldehyde from l-phenylalanine with a mutant form of 4-hydroxymandelate synthase. Biosci Biotechnol Biochem. 2022, 86(12):1718–1725. http://doi.org:10.1093/bbb/zbac162

19. Hubbard BK, Thomas MG, Walsh CT. Biosynthesis of L-p-hydroxyphenylglycine, a non-proteinogenic amino acid constituent of peptide antibiotics. Chem Biol. 2000, 7(12):931–942. http://doi.org:10.1016/S1074-5521(00)00043-0

20. Reifenrath M, Boles E. Engineering of hydroxymandelate synthases and the aromatic amino acid pathway enables *de novo* biosynthesis of mandelic and 4-hydroxymandelic acid with *Saccharomyces cerevisiae*. Metab Eng. 2018, 45:246–254. http://doi.org:10.1016/j.ymben.2018.01.001

21. Huang H-R, Xu J-H. Preparation of (*S*)-mandelic acid from racemate using growing cells of Pseudomonas putida ECU1009 with (*R*)-mandelate degradation activity. Biochem Eng J. 2006, 30(1):11–15. http://doi.org:10.1016/j.bej.2006.01.010

22. Koszelewski D, Tauber K, Faber K, Kroutil W. omega-Transaminases for the synthesis of non-racemic alpha-chiral primary amines. Trends Biotechnology. 2010, 28(6):324–332. http://doi.org:10.1016/j.tibtech.2010.03.003

23. Wu J, Du G, Zhou J, Chen J. Metabolic engineering of *Escherichia coli* for (2S)-pinocembrin production from glucose by a modular metabolic strategy. Metab Eng. 2013, 16:48–55. http://doi.org:https://doi.org/10.1016/j.ymben.2012.11.009

24. Yang X, Wang C, Yin J, Wang J, Zhao D, Zhang J, Gao H. *De novo* biosynthesis of phenylpyruvic acid by engineered *Escherichia coli*. Biosci Biotechnol Biochem. 2026, 90(7):958–970. http://doi.org:10.1093/bbb/zbag050

25. Tina L-E, Gregory S. Feedback inhibition of chorismate mutase/prephenate dehydrogenase (TyrA) of *Escherichia coli*: generation and characterization of tyrosine-insensitive mutants. Appl Environ Microbiol. 2005, 71(11):7224–7228. http://doi.org:10.1128/AEM.71.11.7224-7228.2005

26. Lütke-Eversloh T, Stephanopoulos G. Combinatorial pathway analysis for improved L-tyrosine production in *Escherichia coli* : Identification of enzymatic bottlenecks by systematic gene overexpression. Metab Eng. 2007, 10(2):69–77. http://doi.org:10.1016/j.ymben.2007.12.001

27. Chen Y, Weihong J, Yingmiao L, Bingbing S, Lixia L, Yuanyuan N, Zhoutong S, Sheng Y. Metabolic engineering of the L-phenylalanine pathway in

Escherichia coli for the production of S- or R-mandelic acid. Microb Cell Fact. 2011, 10(1):71. http://doi.org:10.1186/1475-2859-10-71

28. Alberto R, A MJ, Noemí F, Adelfo E, Guillermo G, Francisco B. Engineering *Escherichia coli* to overproduce aromatic amino acids and derived compounds. Microb Cell Fact. 2014, 13(1):126. http://doi.org:10.1186/s12934-014-0126-z

29. Fujiwara R, Noda S, Tanaka T, Kondo A. Metabolic engineering of *Escherichia coli* for shikimate pathway derivative production from glucose-xylose co-substrate. Nat Commun. 2020, 11(1):279. http://doi.org:10.1038/s41467-019-14024-1

30. Van Der Donk WA, Zhao H. Recent developments in pyridine nucleotide regeneration. Curr Opin Biotechnol. 2003, 14(4):421–426. http://doi.org:10.1016/s0958-1669(03)00094-6

31. Lee S, Kim M, Ahn BJ, Jang Y. Odorant-responsive biological receptors and electronic noses for volatile organic compounds with aldehyde for human health and diseases: A perspective review. J Hazard Mater. 2023, 455:131555. http://doi.org:10.1016/j.Jhazmat.2023.131555

32. Burg JM, Cooper CB, Ye Z, Reed BR, Moreb EA, Lynch MD. Large-scale bioprocess competitiveness: the potential of dynamic metabolic control in two-stage fermentations. Curr Opin Chem Eng. 2016, 14:121–136. http://doi.org:10.1016/j.coche.2016.09.008

832 33. Gao C, Tang W, Guo L, Hu G, Liu J, Liu L, Chen X. Improving succinat
833 e production by engineering oxygen-dependent dynamic pathway regulation
834 in *Escherichia coli*. Syst Microbiol Biomanuf. 2021, 2(2):1–14. http://doi.org:
835 10.1007/s43393-021-00065-5
836

Supplementary Files

This is a list of supplementary files associated with this preprint. Click to download.

- Supportinginformation.docx